Low-Threshold Strain-Compensated InGaAs(N) ($\lambda = 1.19$–1.31 μm) Quantum-Well Lasers

Nelson Tansu and Luke J. Mawst, *Senior Member, IEEE*

***Abstract*—Highly strained ($\Delta a/a \sim 2.5\%$) $In_{0.4}Ga_{0.6}As$- and $In_{0.4}Ga_{0.6}As_{0.995}N_{0.005}$-quantum-well (QW) active lasers utilizing strain-compensating InGaP–GaAsP buffer layers and $GaAs_{0.85}P_{0.15}$ barrier layers, grown by metal–organic chemical vapor deposition (MOCVD), are demonstrated with lasing emission wavelength of 1.185 and 1.307 μm, respectively. Threshold and transparency current density for the strain compensated InGaAsN QW lasers, with emission wavelength of 1.295 μm, are measured to be as low as 290 A/cm^2 ($L = 1500$ μm) and 110 A/cm^2, respectively, with characteristic temperature of T_o and T_1 of 130 K and 400 K.**

***Index Terms*—Diode lasers, epitaxial growth, InGaAs–GaAs, InGaAsN–GaAs, quantum-well lasers, semiconductor lasers, strain.**

I. Introduction

THE USE of an InGaAsN quantum-well (QW) active region on a GaAs substrate, to achieve 1.3-μm temperature-insensitive diode lasers, have been proposed by Kondow, *et al.* [1]. Since then, there have been many efforts [1]–[15] in pushing the wavelength emission near 1.3 μm on GaAs substrates by using highly strained InGaAsN QW-active.

In this letter, we report studies on high-compressive strain InGaAs(N)-QW active region lasers with strain-compensating barrier and buffer layers, aimed for emission wavelength between 1.19–1.31 μm. Besides our previous work on $In_{0.35}Ga_{0.65}As$ QW ($\lambda = 1.17$ μm) lasers [4], the strain compensation of InGaAs(N) QW lasers ($\lambda > 1.17$ μm) using GaAsP tensile-strained barriers has been reported by [5], [6], [13], [14].

In the present work, we report a comparison study of strain compensated $In_{0.4}Ga_{0.6}As$ and $In_{0.4}Ga_{0.6}As_{0.995}N_{0.005}$ QW lasers with emission wavelengths of 1.19 μm and 1.29–1.31 μm, respectively. The optical luminescence of the high-In-content (40% In) InGaAs QWs, in structures (in Fig. 1) with high Al-content AlGaAs lower cladding layers, are significantly improved through the use of an InGaP–GaAsP buffer layer.

II. Laser Structures With Tensile-Strained Buffer

The lasers structures utilized here, shown in Fig. 1, were grown by low-pressure metal–organic chemical vapor deposition (MOVCD). Trimethylgallium (TMGa), trimethylaluminum (TMAl) and trimethylindium (TMIn) are used as the group III sources and AsH_3, PH_3, and U-dimethylhydrazine (U-DMHy) are used as the group V sources. The dopants used here are SiH_4 and Dielthylzinc (DEZn) for the n- and p-dopants, respectively.

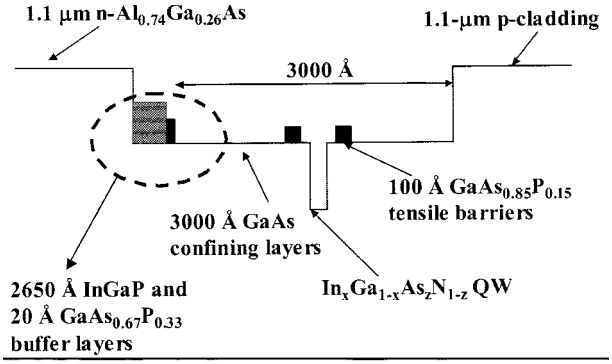

	Laser A	Laser B	Laser C
QW	$In_{0.35}Ga_{0.65}As$	$In_{0.4}Ga_{0.6}As$	$In_{0.4}Ga_{0.6}As_{0.995}N_{0.005}$
t_{QW} (Å)	79	60	60
Barriers	$GaAs_{0.85}P_{.15}$	$GaAs_{0.85}P_{.15}$	$GaAs_{0.85}P_{.15}$
p-cladding	p-$In_{0.48}Ga_{0.52}P$	p-$Al_{0.74}Ga_{0.26}As$	p-$Al_{0.74}Ga_{0.26}As$
λ(μm)	1.170	1.185	1.305

Fig. 1. Schematic energy bandgap diagram for the InGaAs(N)–GaAsP–GaAs QW laser structure. The table describes the various lasers structures studied.

All laser structures studied here use strain compensation by $GaAs_{0.85}P_{0.15}$ tensile-strained barriers, as shown in Fig. 1 [4]. Laser structure A, previously reported [4], is also shown in Fig. 1 for comparison purposes. This structure contains an 80-Å $In_{0.35}Ga_{0.65}As$ QW, resulting in a lasing emission wavelength of $\lambda = 1.17$ μm. The lower and upper cladding layers are based on n-$Al_{0.85}Ga_{0.15}As$ and p-$In_{0.48}Ga_{0.52}P$, respectively. Buffer layers of 2650-Å n-InGaP ($\Delta a/a = +1500$ ppm), and 20-Å highly-tensile $GaAs_{0.67}P_{0.33}$ ($\Delta a/a = -1.2\%$) are also inserted between the lower AlGaAs cladding and the GaAs waveguide layers. The second (B) and third (C) laser structures have active regions consisting of a 60-Å $In_{0.4}Ga_{0.6}As$ QW, and 60-Å $In_{0.4}Ga_{0.6}As_{0.995}N_{0.005}$ QW, respectively, both with an n-$Al_{0.74}Ga_{0.26}As$ lower cladding layer and a slightly tensile-strained ($\Delta a/a = -700$ ppm) n-InGaP and $GaAs_{0.67}P_{0.33}$ buffer layers. The top cladding layer of lasers B and C are based on 1.1-μm thick 725 °C-grown and 640 °C-grown p-$Al_{0.74}Ga_{0.26}As$ layers, respectively.

The use of a tensile-strained InGaP–GaAsP buffer layers is found to be critical for the growth of the highly strained InGaAs(N) QW active region, when high Al-content AlGaAs cladding layers are utilized. Room-temperature PLs for a 60-Å $In_{0.4}Ga_{0.6}As$ QW ($\lambda_{peak} = 1.2$ μm), grown on a 1.1-μm-thick n-$Al_{0.85}Ga_{0.15}As$ bottom-cladding layer, with a tensile-strained

Manuscript received October 23, 2001; revised December 10, 2001.

The authors are with the Reed Center for Photonics, Department of Electrical Computer Engineering, University of Wisconsin-Madison, Madison, WI 53706-1691 USA (e-mail: tansu@cae.wisc.edu).

Publisher Item Identifier S 1041-1135(02)01858-X.

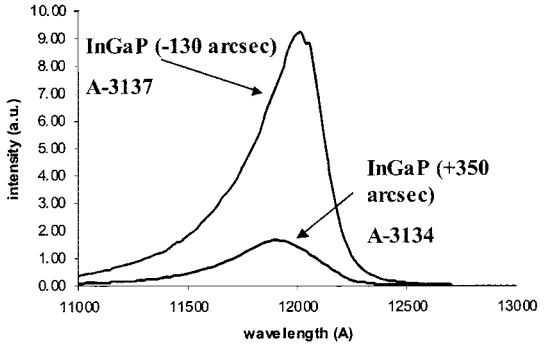

Fig. 2. The room-temperature photoluminescence of the $In_{0.4}Ga_{0.6}As$–$GaAs_{0.85}P_{0.15}$ QW, on a 1.1-μm-thick high Al-content n-AlGaAs bottom cladding layer, with various InGaP buffer.

TABLE I
PERFORMANCE AND INTRINSIC DEVICE PARAMETERS OF $In_{0.35}Ga_{0.65}As$ QW (A), $In_{0.4}Ga_{0.6}As$ QW (B), AND $In_{0.4}Ga_{0.6}As_{0.995}N_{0.005}$ (C) DIODE LASERS WITH 100-μm STRIPE-WIDTH DEVICES

	Laser A $In_{0.35}Ga_{0.65}As$	Laser B $In_{0.4}Ga_{0.6}As$	Laser C $In_{0.4}Ga_{0.6}As_{0.995}N_{0.005}$	
L(μm)	1000	1000	750	1500
t_{QW} (Å)	80	60	60	60
λ(μm)	1.170	1.185	1.290	1.295
J_{th} (A/cm^2)	70	130	400	289
J_{tr} (A/cm^2)	30	59	110	110
η_d (%)	50	53	51	40
η_i (%)	60	79	72	72
α_i (cm^{-1})	2	6	6	6
g_o(cm^{-1})	1975	1600	1120	1120
T_0 (K)	120	200	110	130
T_1 (K)	325	750	416	400

($\Delta a/a = -700$ ppm) and a compressively strained ($\Delta a/a = +1500$ ppm) InGaP in addition to the $GaAs_{0.67}P_{0.33}$ buffer layer, as shown in Fig. 2 indicate improved (up to five times) luminescence of the $GaAs_{0.67}p_{0.33}$ buffer layer, as tensile InGaP buffer. By comparison, we find similar structures without the buffer layers, exhibit extremely poor optical luminescence. Further studies are still required to understand the role of these buffer layers in the improvement of the optical luminescence of the $In_{0.4}Ga_{0.6}As$ QW.

III. InGaAs(N)-QW LASER CHARACTERISTICS

Broad-area lasers with stripe width of 100 μm are fabricated to characterize the device performance. The intrinsic physical device parameters can then be extracted from length dependent studies performed on these lasers. All the measured parameters for these lasers are summarized in Table I.

The laser structure A, which has the top cladding of p-InGaP, suffers from low current injection efficiency ($\eta_i = 60\%$) [4]. Temperature-dependent measurements of η_i indicate carrier leakage to the cladding layers is not responsible for the low internal efficiency [15]. By replacing the top cladding of p-InGaP with p-AlGaAs, significantly higher efficiency ($\eta_i = 80\%$) is observed in laser B. Similar observations of improvement in the injection efficiency, by changing both cladding layers from InGaP to AlGaAs material, was recently reported by Kondo *et al.* [3]. Here, we have identified the upper cladding layer/waveguide interface as a region of high nonradiative recombination. The observed improvement in the $\eta_i$in laser B can then be attributed to the elimination of the interface between GaAs and p-InGaP, which contributes significantly to carrier leakage through interfacial defects. The transparency current density ($J_{tr} = 59$ A/cm^2) of laser B is slightly increased compared to that ($J_{tr} = 30$ A/cm^2) of laser A, which is consistent with the observation that the PL intensity of the $In_{0.4}Ga_{0.6}As$ QW is approximately a half of that of $In_{0.35}Ga_{0.65}As$ QW. The reduction of optical luminescence intensity of the $In_{0.4}Ga_{0.6}As$ QW is presumably due to a reduction in the crystal quality of the higher In content InGaAs QW used in laser B. Nevertheless, very low threshold current density ($J_{th} = 100$ A/cm^2, $L = 2000$ μm) and high external differential quantum efficiency ($\eta_d = 63\%$, $L = 500$ μm) are obtained for laser B, with $\lambda = 1.185$ μm.

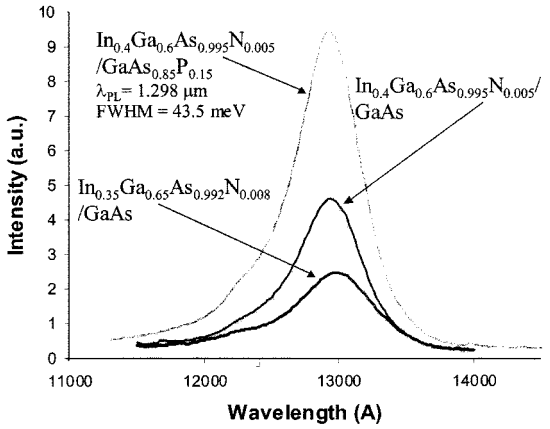

Fig. 3. The room-temperature photoluminescence of the strain-compensated $In_{0.4}Ga_{0.6}As_{0.995}N_{0.005}$–$GaAs_{0.85}P_{0.15}$ QW, and the uncompensated $In_{0.4}Ga_{0.6}As_{0.995}N_{0.005}$ QW and $In_{0.35}Ga_{0.65}As_{0.992}N_{0.008}$ QW.

A comparison of room-temperature PL for three different InGaAsN QW samples, without post-growth annealing, is shown in Fig. 3. The luminescence intensity of the $In_{0.4}Ga_{0.6}As_{0.995}N_{0.005}$ QW is significantly stronger than that of the $In_{0.35}Ga_{0.65}As_{0.992}N_{0.008}$ QW, presumably due the less N content required to achieve 1.3-μm emission for the higher indium containing QW. By employing strain compensating $GaAs_{0.85}P_{0.15}$tensile-strained ($\Delta a/a = -0.54\%$) barriers in the $In_{0.4}Ga_{0.6}As_{0.995}N_{0.005}$ QW structure, further improvement in the optical luminescence intensity is achieved, presumably due to improved crystal quality of QW material. The use of GaAsP tensile-strained barriers to improve the luminescence of GS-MBE grown InGaAsN QW, at $\lambda = 1.22$ μm, has also been reported by Li, *et al.* [14].

Laser C, which has an active region consisting of a 60-Å $In_{0.4}Ga_{0.6}As_{0.995}N_{0.005}$ QW with $GaAs_{0.85}P_{0.15}$ barriers, exhibits lasing with threshold (J_{th}) and transparency current densities (J_{tr}) of 290 A/cm^2 ($L = 1500$ μm) and 110 A/cm^2, with emission wavelength of 1.295 μm. For shorter cavity length ($L = 750$ μm) InGaAsN QW lasers, with $\lambda = 1.29$ μm, low threshold current density ($J_{th} = 400$ A/cm^2) and high external differential efficiency ($\eta_d = 51\%$) are also achieved. The threshold and transparency current density of our InGaAsN QW lasers are among the lowest values reported for InGaAsN QW

lasers [7]–[11], [13] with $\lambda \sim 1.28$–1.3 μm. The higher $J_{\rm tr}$ of the InGaAsN QW, compared with that of the InGaAs QW, may result from the higher O and C impurity levels, which would contribute to the nonradiative recombination in QW. The large variation in the $J_{\rm th}$ may be attributed to the variations in composition of the buffer layer across the wafer, since the optical luminescence was found to be very sensitive to the strain of the buffer layers. Current annealing, which has been previously reported [8], reduces the $J_{\rm th}$ of our InGaAsN lasers by approximately 20%–25% from the initial values. We do not observe any changes in the η_d or emission wavelength between annealed and unannealed devices. The fact, that the current annealing process does not alter the η_d, indicates that the improvement in $J_{\rm th}$ is solely due to a decrease in the non-radiative recombination rate, which will in turn lead to a reduction in $J_{\rm tr}$. The lateral and transverse full-width at half-maximum (FWHM) far-field angles are measured as 7° and 54°, respectively.

The measured η_i of lasers B and C are 80 and 72%, respectively. The differences in η_i between the structures is still under study, and could be either the result of the large scatter in the data for the InGaAsN QW lasers or some other mechanisms. The material-gain-parameter, g_o, for lasers B and C are measured to be 1600 cm^{-1} and 1120 cm^{-1}, respectively.

IV. Temperature Characteristics of InGaAs(N) QW

Characterization of the broad-area lasers are performed in temperature range of 20°C–60 °C, under pulsed operation to determine the characteristic temperature coefficients of the threshold current density (T_o) and external differential quantum efficiency (T_1). The T_o and T_1 values for laser B are significantly higher compared to those of laser A, due to the reduced recombination in SCH in laser B. The T_o values for laser B are measured to be in range of 180 K–200 K for 500–2000 μm cavity length devices. The T_1 values for laser B are measured to be 1000 K, 750 K, and 410 K, respectively, for 500-, 1000-, and 2000-μm cavity length devices. We observe the expected length dependence to the T_0 and T_1, due to the variation of threshold gain with cavity length [15].

Laser C, which employs the $In_{0.4}Ga_{0.6}As_{0.995}N_{0.005}$ QW with emission wavelength of 1.29–1.307 μm, also exhibits low temperature sensitivity. The T_o and T_1 values for 1500-μm cavity lengths are 130 K and 400 K, respectively. These values are high compared to previously reported values for InGaAsN-QW lasers at $\lambda = 1.3$ μm [7]–[11], and reflect the strong active-layer carrier confinement due to the GaAsP barrier layers and high-Al content AlGaAs cladding layers.

V. Conclusion

We have demonstrated very low threshold ($J_{\rm th} = 100$ A/cm^2, $L = 2000$ μm) and transparency ($J_{\rm tr} = 59$ A/cm^2) current density diode lasers utilizing strain-compensated 60-Å $In_{0.4}Ga_{0.6}As$–$GaAs_{0.85}P_{0.15}$ QW, with lasing emission wavelength of 1.185 μm. High internal ($\eta_i = 80\%$) and external differential quantum efficiencies ($\eta_d = 63\%$, $L = 500$ μm) have also been achieved. The increase in the η_i, over previously reported structures, is attributed to the use of a p-AlGaAs, in place of p-InGaP, as the top cladding layer.

MOCVD-grown strain-compensated 60-Å $In_{0.4}Ga_{0.6}As_{0.995}N_{0.005}$–$GaAs_{0.85}P_{0.15}$ QW, with lasing emission wavelength of 1.295 μm, exhibits extremely low threshold ($J_{\rm th} = 290$ A/cm^2, $L = 1500$ μm) and transparency current density ($J_{\rm tr} = 110$ A/cm^2) with high external ($\eta_d = 51\%$, $L = 750$ μm) differential quantum efficiency. Both $In_{0.4}Ga_{0.6}As$ and $In_{0.4}Ga_{0.6}As_{0.995}N_{0.005}$ QW lasers demonstrate low temperature sensitivity of the threshold current density and the external differential quantum efficiency.

Acknowledgment

The authors would like to acknowledge helpful technical discussions with Dr. M. R. T. Tan, Dr. D. P. Bour, and Dr. S. W. Corzine at Agilent Technologies.

References

[1] M. Kondow, T. Kitatani, S. Nakatsuka, M. C. Larson, K. Nakahara, Y. Yazawa, M. Okai, and K. Uomi, "GaInNAs: A novel material for long wavelength semiconductor lasers," *IEEE J. Select. Topic Quantum Electron.*, vol. 3, pp. 719–730, June 1997.

[2] S. Sato and S. Satoh, "1.21 μm continuous-wave operation of highly strained GaInAs quantum well lasers on GaAs substrates," *Jpn. J. Appl. Phys.*, vol. 38, pp. L990–L992, 1999.

[3] T. Kondo, D. Schlenker, T. Miyamoto, Z. Chen, M. Kawaguchi, E. Gouardes, F. Koyama, and K. Iga, "Lasing characteristics of 1.2 μm highly strained GaInAs/GaAs quantum well lasers," *Jpn. J. Appl. Phys.*, vol. 40, pp. 467–471, Feb. 2000.

[4] N. Tansu and L. J. Mawst, "High-performance, strain compensated InGaAs–GaAsP–GaAs ($\lambda = 1.17\mu$m) quantum well diode lasers," *IEEE Photon. Technol. Lett.*, vol. 13, pp. 179–181, Mar. 2001.

[5] W. Choi, P. D. Dapkus, and J. J. Jewell, "1.2-μm GaAsP/InGaAs strain compensated single-quantum well diode laser on GaAs using metal–organic chemical vapor deposition," *IEEE Photon. Technol. Lett.*, vol. 11, pp. 1572–1574, Dec. 1999.

[6] F. Bugge, G. Erbert, J. Fricke, S. Gramlich, R. Staske, H. Wenzel, U. Zeimer, and M. Weyers, "12 W continuous-wave diode lasers at 1120 nm with InGaAs quantum wells," *Appl. Phys. Lett.*, vol. 79, no. 13, pp. 1965–1967, Sept. 2001.

[7] S. Sato, "Low threshold and high characteristics temperature 1.3 μm range GaInNA's lasers grown by metalorganic chemical vapordeposition," *Jpn. J. Appl. Phys.*, vol. 39, pp. 3403–3405, June 2000.

[8] M. Kawaguchi, T. Miyamoto, E. Gouardes, D. Schlenker, T. Kondo, F. Koyama, and K. Iga, "Lasing characteristics of low-threshold GaInNA's lasers grown by metalorganic chemical vapor deposition," *Jpn. J. Appl. Phys.*, vol. 40, pp. L744–L746, July 2001.

[9] F. Hohnsdorf, J. Koch, S. Leu, W. Stolz, B. Borchert, and M. Druminski, "Reduced threshold current densities of (GaIn)(Nas)/GaAs single quantum well lasers for emission wavelengths in the range 1.28–1.38 μm," *Electron. Lett.*, vol. 35, no. 7, pp. 571–572, 1999.

[10] B. Borchert, A. Y. Egorov, S. Illek, and H. Riechert, "Static and dynamics characteristics of 1.29 μm GaInNA's ridge-waveguide laser diodes," *IEEE Photon. Technol. Lett.*, vol. 12, pp. 597–599, June 2000.

[11] M. R. Gokhale, P. V. Studenkov, J. Wei, and S. R. Forrest, "Low-threshold current, high efficiency 1.3-μm wavelength aluminum-free InGaAsN-based quantum-well lasers," *IEEE Photon. Technol. Lett.*, vol. 12, pp. 131–133, Feb. 2000.

[12] C. W. Coldren, M. C. Larson, S. G. Spruytte, and J. S. Harris, "1200 nm GaAs-based vertical cavity lasers employing GaInNA's multiquantum well active regions," *Electron. Lett.*, vol. 36, no. 11, pp. 951–952, 2000.

[13] S. R. Kurtz, R. M. Sieg, A. A. Allerman, K. D. Choquette, and R. L. Naone, "MOCVD-grown, 1.3 μm InGaAsN multiple quantum well lasers incorporating GaAsP strain-compensation layers," in *Proc. SPIE—Photonics West 2001*, vol. 4287, 2001, pp. 170–175.

[14] W. Li, J. Turpeinen, P. Melanen, P. Savolainen, P. Uusimaa, and M. Pessa, "Effects of rapid thermal annealing on strain-compensated GaInNAs/GaAsP quantum well structures and lasers," *Appl. Phys. Lett.*, vol. 78, pp. 91–92, 2001.

[15] N. Tansu, Y. L. Chang, T. Takeuchi, D. P. Bour, S. W. Corzine, M. R. T. Tan, and L. J. Mawst, "Temperature analysis and characteristics of highly-strained InGaAs(N)–GaAsP–GaAs ($\lambda > 1.17$ μm) quantum well lasers," *IEEE. J. Quantum Electron.*, submitted for publication.